PATTERNING SURFACES BY SELF-ORGANIZED GROWTH

KLAUS KERN
Max-Planck-Institut für Festkörperforschung, D-70569 Stuttgart, Germany, and Institut de Physique Expérimentale, EPFL, CH-1015 Lausanne, Switzerland

Abstract. Much effort has been devoted to create semiconductor and metal nanostructures at surfaces. Their controlled fabrication, in particular the creation of lateral order, however, remains an experimental challenge. In this contribution we discuss the fabrication of nanostructures via self-organized growth at surfaces. Advantages and limitations of diffusion controlled molecular beam epitaxy are discussed and novel routes for the fabrication of ordered nanostructures are presented.

1. Introduction

The physical and chemical properties of low-dimensional structures are unique functions of their size and shape and differ significantly from the behavior of bulk matter. Particularly fascinating phenomena occur if the nanostructures are subject to lateral boundary conditions on a length scale where quantum behavior prevails; magnetic nanostructures can be made out of traditionally non-magnetic elements, catalytic activity can emerge, and new electronic quantum devices can be built. Much effort has been devoted to the fabrication of nanostructures at semiconductor and metal surfaces. Arbitrary atomic scale structures could be assembled with the tip of a scanning tunneling microscope (STM) [1], either through direct displacement of atoms, or through tip-assisted decomposition of chemical species. The principal drawback of scanning probe based methods is their serial character. Approaches where a large abundance of structures can be created in parallel are self-organized growth [2], either in the kinetic, or in the thermodynamic regime, and the controlled deposition of size selected clusters from the gas phase [3]. In the kinetic growth regime the hierarchy of activated surface motion can be used to translate random motion into

M. Kotrla et al. (eds.), Atomistic Aspects of Epitaxial Growth, 207–219.

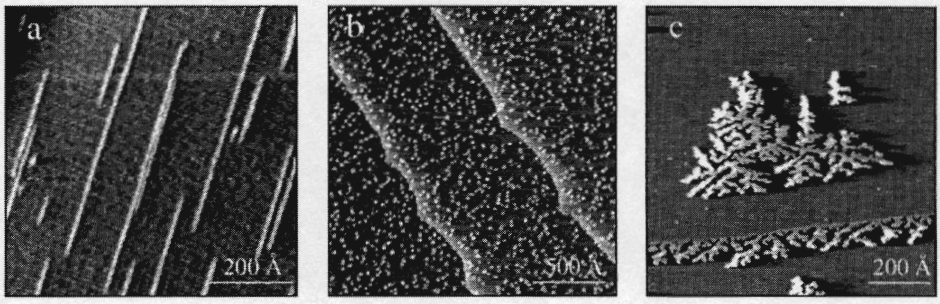

Figure 1. Atomic architecture at surfaces in the kinetic growth regime. (a) Formation of monatomic Cu chains on Pd(110). (b) and (c) Ag nanostructures on Pt(111), size and shape have been determined by controlling the kinetic growth parameters deposition, flux, and temperature.

geometrical order. By exploiting the dependence of the mobility of adsorbed atoms on substrate crystal face and temperature, we are able to grow one- and two-dimensional metal nanostructures with a great variety of forms and sizes (Fig. 1). While the cluster deposition technique produces nearly monodispersed nanostructures at surfaces the self-organized growth suffers from a non-negligible width of the size distribution. In addition, both methods suffer from the statistics inherent in the deposition process leading to largely uncorrelated spatial distributions.

2. Nanostructure Arrays

We have developed a novel route for the fabrication of two-dimensional nanostructure arrays which overcomes these drawbacks [4]. The method is based on confined nucleation on substrates with periodic dislocation networks. Dislocations are found to be strongly repulsive towards diffusing adatoms. For a well-defined set of growth parameters the adatoms are therefore confined within the network unit cells nucleating exactly one island per unit cell. With this method we have grown two-dimensional periodic arrays of Ag, Co and Fe nanostructures.

Figure 2(a) shows the growth template, the equilibrium structure of the second monolayer (ML) of Ag on Pt(111) [5]. The lattice constant of Ag is 4.3% larger than the that of Pt. In the second Ag ML, the compressive strain resulting from this lattice mismatch is relieved in a trigonal network of dislocations with a periodicity of 25 atoms. The dislocations form transitions from fcc to hcp stacking. In contrast to comparable reconstructions, where dislocations run parallel, here the dislocations cross each other, allowing for isotropic strain relief on a small length scale. Larger areas of the energetically favored fcc stacking with respect to hcp stacking areas

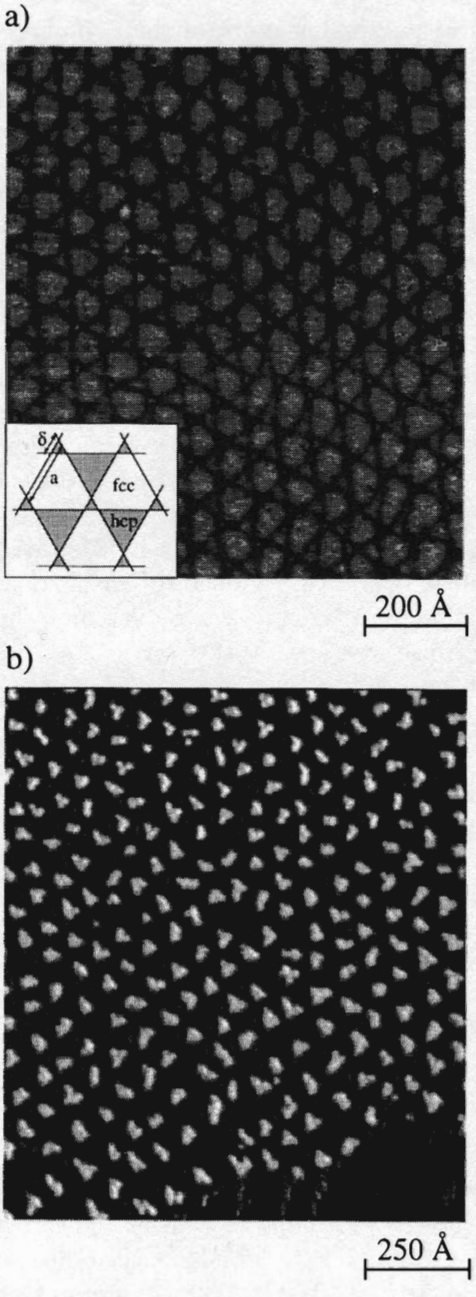

Figure 2. (a) STM image of the (25×25) dislocation network formed by the second Ag monolayer on Pt(111) upon deposition at 400 K and subsequent annealing to 800 K. The inset shows a model of this trigonal strain relief pattern. (b) A superlattice of islands is formed upon Ag deposition to a (coverage $\theta = 0.10$ ML onto this network at 110 K.

are achieved by displacing one class of domain walls by an offset [inset to Fig. 2(a)] relative to the crossing point of the two others. This results in a pattern with trigonal symmetry. Each unit cell shows a large quasi-hexagon with fcc stacking and two triangles of different size with hcp stacking; for details of this strain relief pattern the reader is referred to Ref. [5].

Ag nucleation onto this network at low temperature leads to a high density of islands [Fig. 3(a)]. Only a few of these islands are located near the dislocations. This implies that dislocations constitute repulsive barriers towards diffusing adatoms. With increasing temperatures, the island density approaches a stationary value between 100 K to 130 K, where exactly one island forms per network unit cell [see Figs. 2(b) and 3(b)]. All of the islands nucleate within the distorted hexagons. This implies preferential binding to fcc-areas, in agreement to theory. Hence, atoms landing in one of the two hcp triangles can diffuse into the fcc hexagons but not vice versa. Due to the repulsive nature of the dislocations and the attraction towards specific sites within the unit cell, the periodicity of the dislocation network is congruently transferred to an island superlattice. For growth temperatures of 140 K or above, the island density decreases again. Here, the adatoms thermal energy is sufficient to overcome the repulsive barriers and the Ag atoms diffuse over several superstructure cells before nucleating [Fig. 3(c)].

An interesting side-effect of the ordered nucleation in the intermediate temperature range is an enhanced size uniformity. Atoms deposited into a network unit cell stay confined to this cell by the surrounding dislocations. In the limit of completely repulsive edges of the supercells, sufficiently high mobility of the atoms to ensure nucleation of only one island, and not too high coverages which guaranties that the deposition processes into different supercells are independent events, the size distribution of the island (number of atoms in the islands) is

$$P_k = \binom{n}{k} p^k q^{n-k},$$

where $p = \theta$, $q = 1 - \theta$, with k being the island size n the size of the unit cell and θ the coverage. For our case of $p = 0.1$ and $n = 625$, the binomial distribution has a relative standard deviation (normalized to the average island size) of $\sigma = (q/np)^{1/2} = 0.12$. Due to the convolution of tip and island shape there is a residual width, which explains our larger experimental value of $\sigma = 0.20$. This value represents an upper bound to the real size distribution. The formula of the relative standard deviation evinces the potential of the method: In a system with a superstructure unit cell as large as in the present case, and a coverage of $\theta = 0.5$ ML, one expects a relative width of the size distribution of only 4% in cluster area.

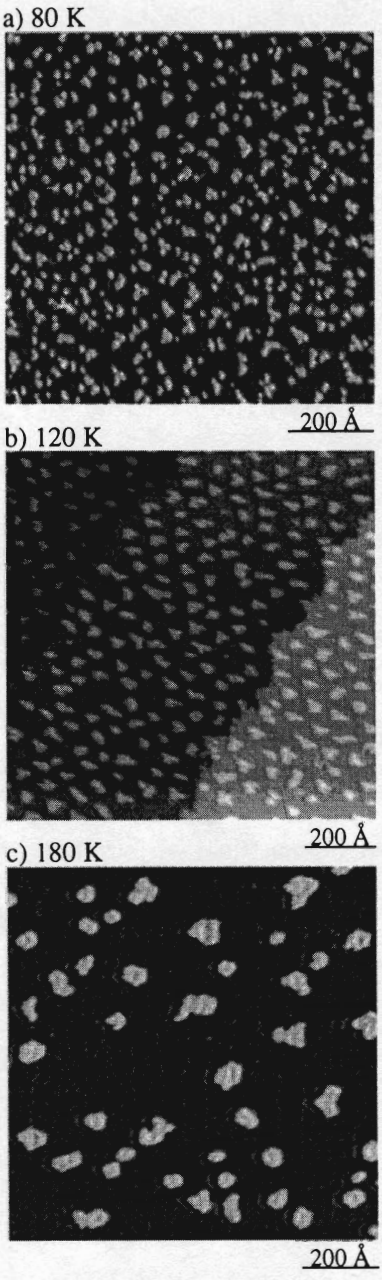

Figure 3. Temperature series of Ag nucleation ($\theta = 0.1$ ML) on the dislocation network of Fig. 1(a). (a) At temperatures below 100 K more than one island nucleates within each unit cell. (b) At temperatures between 100 K and 130 K, ordered nucleation and formation of a superlattice is found. (c) At temperatures above 130 K diffusing adatoms can overcome the repulsive dislocations and the island density drops below one island per unit cell.

In the confined nucleation approach the dislocation network acts as nanotemplate for the growing surface layer. The repulsive interaction between adatoms and dislocations is exploited to nucleate islands only in the center of the unit cell. Dislocations can however also act as attractive trapping sites for adatoms and the preferred nucleation at these traps can also be used to generate ordered two-dimensional nanostructures [6]. One-dimensional arrays of islands (nanowires) can be fabricated by employing periodically stepped surfaces as nanoscale templates. Controlled step decoration is used here to grow the one-dimensional superlattices; nanowires can be grown with atomic precision and periodicities as low as 2 nm [7].

3. Long-Range Adsorbate Interactions

Lateral interactions between adsorbed species have a determining influence on surface processes and might be exploited for structuring in thin film epitaxy. The usually considered interactions range over only a few atomic distances and have amply been studied in the past. However, since more than 20 years stands the theoretical prediction that there should exist adsorbate interactions of extremely long range, mediated by screening in a two-dimensional electron gas [8]. These long range interactions were recently detected by Repp *et al.* [9] and by us [10] for Cu adatoms on the Cu(111) surface. We have investigated two additional adatom systems, namely, Co on Cu(111) and Co on Ag(111) using low-temperature STM. Both metal substrates support a partially filled surface state band at the Fermi energy. The electrons in these surface states form a two dimensional electron gas and are responsible for the interaction predicted by theory. The interaction energy manifests itself up to 60 Å distance, it decays as $1/r^2$ and oscillates with a period reflecting the surface state band structure.

A foreign atom dissolved in a solid, or adsorbed on a surface, imposes its potential onto the host electrons, which they screen by oscillations in their local density of states (LDOS) at the Fermi level (E_F). An example of LDOS oscillations around Cu atoms on a Cu(111) substrate is given in Fig. 4. One realizes that adsorbates can interact through the fact that the adsorption energy of one adsorbate depends on the electron density, which oscillates around the other. Due to the long Fermi-wavelength [e.g., 30 Å for the surface state of Cu(111)] can be extremely long-ranged: Lau and Kohn predicted such oscillatory interactions to depend on distance, r, as $\cos(2k_F r)/r^2$ in the given experimental situation [8].

To map out the long-range interaction of the adsorbates, one has to carefully choose a temperature where diffusion is sufficiently activated so that the adatoms probe the potential in their surroundings, but where they are not too fast that they are trapped by defects or the steps on the surface.

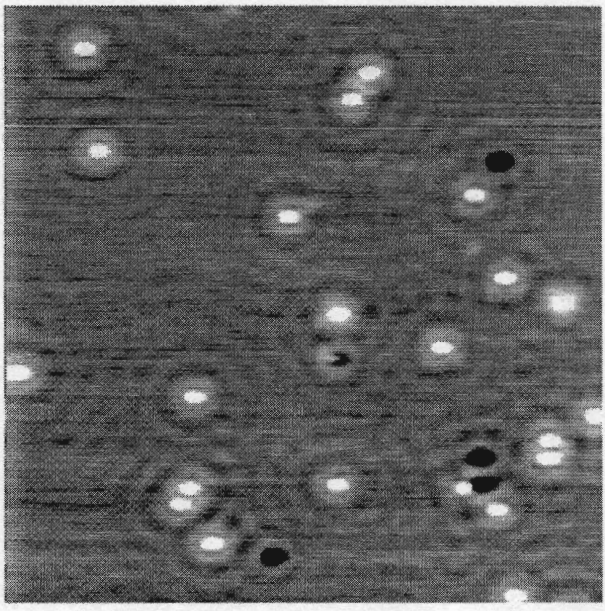

Figure 4. A 35 nm × 35 nm STM image of single Cu atoms (bright spots) on a Cu(111) terrace. The interference pattern in the image are the Friedel-type oscillations of the local density of states due to the localized scatterers (Cu atoms, other defects).

If these conditions are met, then each recorded frame will represent an independent snapshot of the position of the adatoms. Therefore, we studied the diffusion behavior of adatoms of the three mentioned systems. At low temperature standard STM imaging (i.e. with frame rates of 1/100 Hz) can be used to follow the diffusion of, e.g., Cu atoms on the potential landscape of the Cu(111) substrate [10a]. The evaluation of these images results in a plot of the adatom diffusion attempt frequency against temperature determining the diffusion barrier $E_m = 40$ meV and the prefactor $\nu_0 = 10^{12}$ Hz [10].

In regions where there is a low potential adatoms will be found more often than in regions with high potential. Since the potential variations come from other adatoms we produced nearest-neighbor distance histograms (Fig. 5) which show directly the oscillatory behavior of the adsorbate-adsorbate interaction: there are preferred distances between adatoms and less preferred ones. These histograms can be evaluated to directly give the interaction energy $E(r)$, as shown in Fig. 5. We find that $E(r)$ oscillates with a spatial dependence governed by the surface state electrons and that its magnitude is in the meV range. The experimental data are in perfect agreement with theory [11].

The electronic origin of the long-range interactions is unequivocally

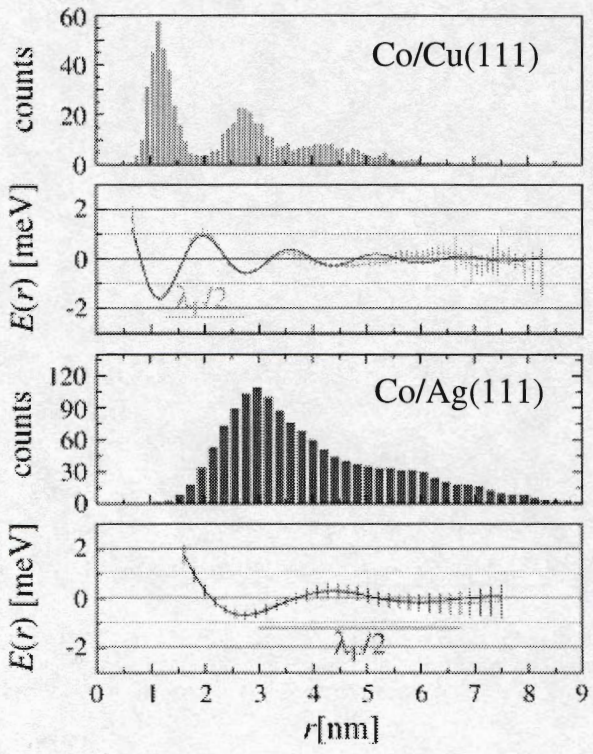

Figure 5. Nearest-neighbor distance histograms and the resulting interaction energy as a function of distance for (a) Co on Cu(111) and (b) Co on Ag(111).

proven by demonstration of the scaling of the interaction length with k_F. The more than two times longer wavelength of the interaction on Ag(111) compared to Cu(111) is evident in Fig. 5. On the copper surface we observe a Co-Co repulsion for $r < 8$ Å and the first minimum in interaction energy at around 12Å, while at the Ag surface these values shift to 20 Å and 27 Å, respectively. Therefore we conclude that the observed long-range interactions are indeed mediated by the nearly-free two-dimensional electron gas of the surface state.

As opposed to short-range interactions, the surface-state-mediated long-range interactions are far less element specific and, therefore, of general significance, since they predominantly reflect the surface state band structure. Despite the fact that the observed interaction energies are small, they are expected to influence every adsorbate/substrate system with small diffusion barriers. The substantial repulsion for dimer formation, e.g., more than 18 meV in the case of Cu/Cu(111) [9,10], can delay nucleation to much higher coverages than in classical nucleation and growth scenarios

[12,13]. These inherent adsorbate interactions might, however, also be used in a constructive way to build self-organized artificial atomic superlattices of various species on metal substrates. These superlattices have a smaller lattice constant than any that could be prepared by other techniques and yet the atoms are far enough apart as to not interact (i.e. bind) directly.

4. Supramolecular Nanostructures

Supramolecular structures formed by the self-assembly of functional molecular building blocks are a promising class of surface supported nanostructures. Particularly useful for their fabrication is hydrogen bonding, which provides both high selectivity and directionality. Hydrogen-bonded architectures are abundant in biological systems, which has motivated their exploitation in supramolecular chemistry. This has been demonstrated particularly for systems in solution, molecular crystals, and for two-dimensional layers [14].

We have demonstrated that novel supramolecular nanostructures can be generated at surfaces on the basis of this concept [15]. For our study we employed 4-[trans-2(pyrid-4-yl-vinyl)] benzoic acid (PVBA), which has been specifically designed for non-linear optics applications. Its planar and rigid molecular structure comprises a pyridyl group as the head and a carboxylic acid group as the tail [Fig. 6(a)] and is ideal for self-assembly by head-to-tail hydrogen bonding. Small amounts of PVBA were evaporated under ultra-high vacuum conditions onto different well-defined single crystal metal surfaces by organic molecular beam epitaxy and in situ characterized by scanning tunneling microscopy.

Molecular self-assembly at surfaces is governed by the subtle balance between intermolecular and molecule-surface interactions. The STM data reproduced in Fig. 6(b-d) demonstrate how self-assembly can be tuned for a given molecule by the choice of substrate material and symmetry. The interaction of PVBA with the transition metal surface Pd(110) is visualized in Fig. 6(b). Strong π-bonding to Pd surface atoms enforces a flat adsorption geometry. Two distinct molecular orientations exist exclusively which allow for the accommodation of the molecular units at sites on the anisotropic substrate with high symmetry. PVBA is immobile at room-temperature and isolated molecules are randomly distributed on the surface. This also holds at higher temperature, where thermal mobility becomes appreciable, which demonstrates the dominance of the adsorbate-substrate interactions with this system. Low-temperature aggregation and growth of dendritic molecular islands is observed on switching to the more inert Cu(111) surface [Fig. 6(c)], which is indicative of a higher surface mobility and larger lateral interactions. However, the adsorption geometry is not unique and flat

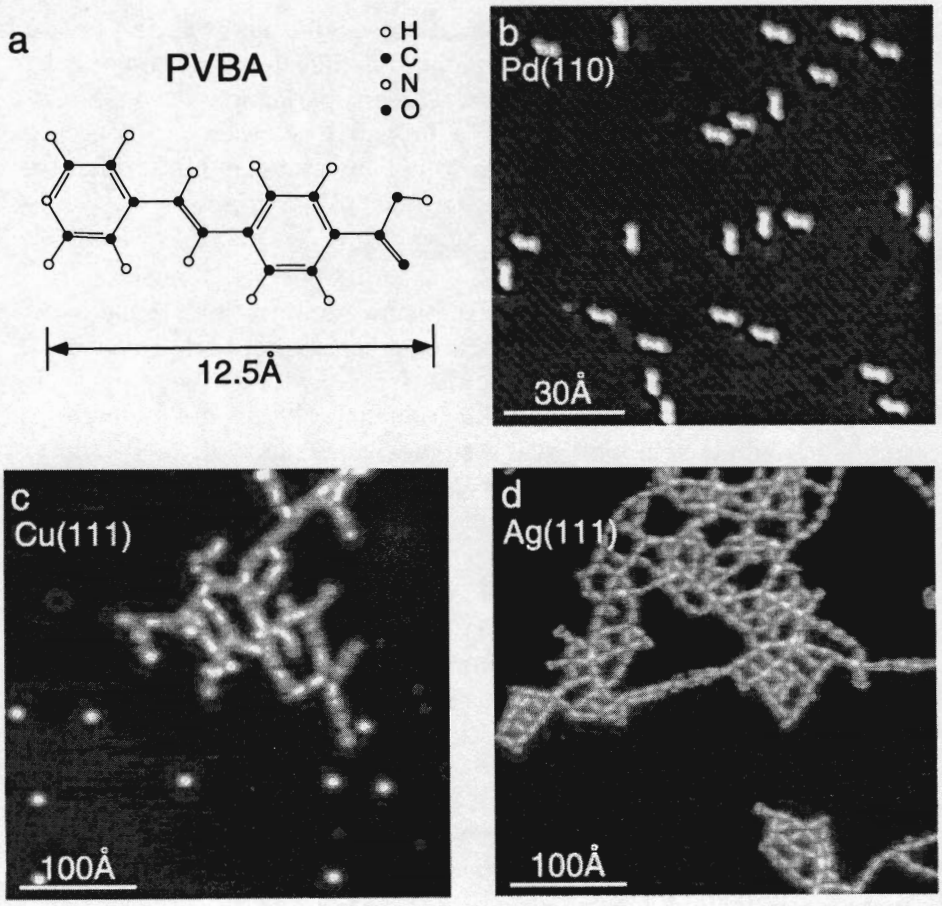

Figure 6. (a) Molecular structure of 4-[trans-2-(pyrid-4-yl-vinyl)] benzoic acid (PVBA) with a pyridyl group at the head and a benzoic acid moiety at the tail. Pictures (b)-(d) show STM topographs of PVBA on different single-crystal metal substrates. (b) Strong adsorbate-substrate interaction on a Pd(110) surface: isolated, immobile PVBA molecules lie flat in two distinct orientations (measured at 325 K) and remain randomly distributed upon annealing at 450 K. (c) On a Cu(111) surface, flat molecules in dendritic islands coexist with isolated molecules in an upright bonding configuration (single protrusions) after adsorption at 160 K. (d) The complex aggregation of PVBA lying flat on Ag(111) reflects the surface mobility and attractive interactions between molecular endgroups at 125 K.

adsorbed molecules coexist with single ones in upright orientations, which are imaged as spherically symmetrical protrusions. The STM topograph in Fig. 6(d) reveals that flat adsorption of PVBA prevails on Ag(111). Again, island formation is already found at low temperatures, and inspection of the island shapes reveals that their formation must be a result of attractive interactions between the molecular endgroups. This observation is in line

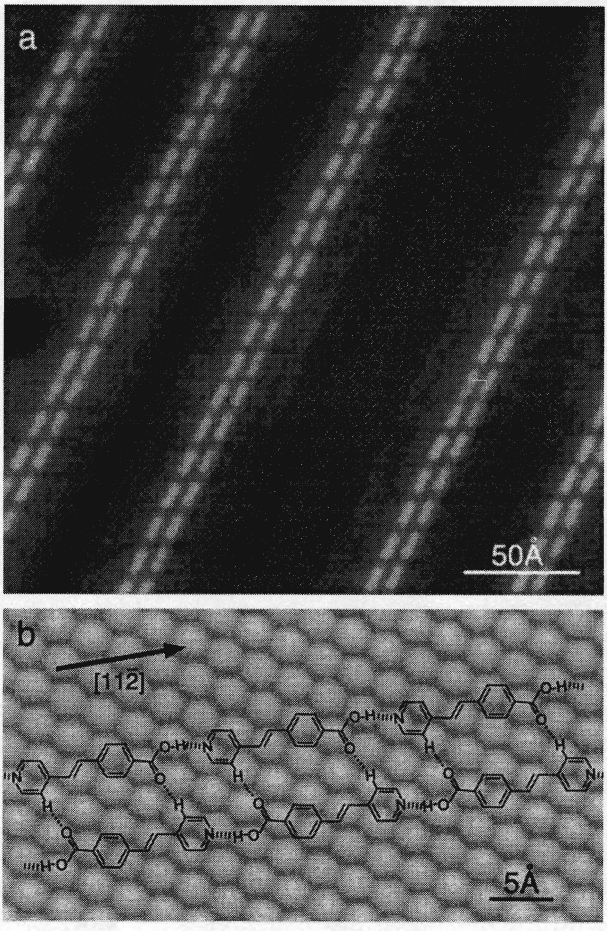

Figure 7. (a) The formation of an one-dimensional supramolecular PVBA superstructure by self-assembly mediated by H-bond formation on an Ag(111) surface at 300 K (measured at 77 K). Twin chains evolve consisting of coupled rows of PVBA molecules. (b) Montage of an atomic-resolution image of Ag(111) with the repeat motif of the PVBA twin chains drawn to scale illustrating the match of the molecular geometry and substrate lattice. The intermolecular interactions, i.e., weak OH–N and possible weak CH–OC hydrogen bonds are indicated.

with the directional interactions expected from the formation of hydrogen bonds.

The observed growth scenario can be considered as a diffusion-limited aggregation of rodlike particles, which is subject to anisotropic interactions. Accordingly, the irregularity of the formed agglomerates suggests that their shape results from kinetic limitations, whereby thermal equilibrium is not attained. The data reproduced in Fig. 7(a) show that well-ordered one-dimensional supramolecular structures evolve on Ag(111) when the thermal

energy is augmented by adsorption or annealing at 300 K. PVBA twin chains are formed which run straight along a $\langle 11\bar{2} \rangle$ direction of the Ag lattice. Due to the substrate symmetry three rotational domains exist. The molecular axis is oriented along the chain direction, in agreement with the expected formation of hydrogen bonds between the PVBA endgroups.

High-resolution STM data allow for the elucidation of fine chain details. Firstly, a slight asymmetry of the molecules becomes apparent signaling that PVBA molecules in adjacent rows are aligned antiparallel. The chain periodicity amounts to 15.0 Å, that is $p = 3\sqrt{3}a$, where a is the Ag(111) surface lattice constant (2.89 Å). The rows of PVBA within the twin chains are shifted by $\Delta p \approx 3.7$ Å with respect to each other. This observation suggests an intricate coupling mechanism between adjacent rows separated by $d \approx 2.4a$.

The observed features of the supramolecular structure can be rationalized by an atomic model. As is illustrated by the repeat motif in Fig. 7(b), the displacement and the antiparallel alignment allow for a complementary assembly of two equivalent PVBA molecules, which are accommodated in similar adsorption geometries. When an unrelaxed molecular configuration is assumed, molecules within a chain are coupled by weak OH–N hydrogen bonds with a length of 2.5 Å. The coupling of the PVBA in adjacent rows is associated with weak intermolecular interactions. In addition to the expected electrostatic interactions between the polar molecules, a weak CH–OC hydrogen bonding is feasible. The geometrical arrangement is a compromise between the lateral intermolecular interaction and the bonding to the substrate. As a result of the inter-row distance of $2.4a$, there is a slight outward relaxation of the rows away from the centers of the hollow-site positions of the Ag(111) substrate lattice. This relaxation and the suggested inward orientation of the C=O group prevent two-dimensional growth and thus account for the directional self-assembly of the twin chain. The rather regular mesoscopic ordering of the supramolecular chains into a nanograting, reminiscent of mesoscopic superstructures induced by relaxation of surface strain [16], can be rationalized by the action of weak, long-range repulsive dipole-dipole interactions between the twin chains [17,18].

Our findings suggest that the self-assembly of properly designed molecules by non-covalent bonding opens up novel avenues for the positioning of functional units in supramolecular architectures at surfaces by organic molecular beam epitaxy. It is believed that this approach will be valuable for the future fabrication of nanoscale devices and supramolecular engineering.

References

1. Eigler, D.M. and Schweizer, E.K. (1990) Positioning single atoms with a scanning tunneling microscope, *Nature* **344**, pp. 524–526.
2. Röder, H., Hahn, E., Brune, H., Bucher, J.P. and Kern, K. (1993) Building one-dimensional and 2-dimensional nanostructures by diffusion-controlled aggregation at surfaces, *Nature* **366**, pp. 141–143.
3. Bromann, K., Felix, C., Brune, H., Harbich, W., Monot, R., Buttet, J. and Kern, K. (1996) Controlled deposition of size-selected silver nanoclusters, *Science* **274**, pp. 956–958.
4. Brune, H., Giovannini, M., Bromann, K. and Kern, K. (1998) Self-organized growth of nanostructure arrays on strain-relief patterns, *Nature* **394**, pp. 451–453.
5. Brune, H., Röder, H., Boragno, C. and Kern, K. (1994) Strain relief at hexagonal-close-packed interfaces, *Phys. Rev. B* **49**, pp. 2997–3000.
6. Chambliss, D., Wilson, R.J. and Chiang, S. (1991) Nucleation of ordered Ni island arrays on Au(111) by surface-lattice dislocations, *Phys. Rev. Lett.* **66**, pp. 1721–1724.
7. Gambardella, P., Blanc, M., Brune, H., Kuhnke, K. and Kern, K. (2000) One-dimensional metal chains on Pt vicinal surfaces, *Phys. Rev. B* **61**, pp. 2254–2262.
8. Lau, K.H. and Kohn, W. (1978) Indirect long-range oscillatory interaction between adsorbed atoms, *Surf. Sci.* **75**, pp. 69–85.
9. Repp, J., Moresco, F., Meyer, G. Rieder, K.-H., Hyldgaard, P. and Persson, M. (2000) Substrate mediated long-range oscillatory interaction between adatoms: Cu/Cu(111), *Phys. Rev. Lett.* **85**, pp. 2981–2984.
10. Knorr, N., Brune, H., Epple, M., Hirstein, A., Schneider, M.A. and Kern, K. (2000) Long-range adsorbate interactions mediated by a two-dimensional electron gas, (submitted).
11. A complete time sequence of such a diffusion study can be watched at `http://www.mpi-stuttgart.mpg.de/KERN/RES_act/supmat_1.html`.
12. Hyldgaard, P. and Persson, M. (2000) Long-ranged adsorbate-adsorbate interactions mediated by a surface-state band, *J. Phys. Cond. Matter* **12**, pp. L13–L19.
13. Bogicevic, A., Ovesson, S., Hyldgaard, P., Lundqvist, B.I., Brune, H and Jennison, D.R. (2000) Nature, strength, and consequences of indirect adsorbate interactions on metals, *Phys. Rev. Lett.* **85**, pp. 1910–1913.
14. Fichthorn, K.A. and Scheffler, M. (2000) Island nucleation in thin-film epitaxy: A first-principles investigation, *Phys. Rev. Lett.* **84**, pp. 5371–5374.
15. Philp, D. and Stoddart, J.F. (1996) Self-assembly in natural and unnatural systems, *Angew. Chem. Int. Ed. Engl.* **35**, pp. 1154–1196.
16. Barth, J.V., Weckesser, J., Cai, C.Z., Gunter, P., Burgi, L., Jeandupeux, O. and Kern, K. (2000) Building supramolecular nanostructures at surfaces by hydrogen bonding, *Angew. Chem. Int. Ed.* **39**, p. 1230.
17. Barth, J.V., Brune, H., Ertl, G. and Behm, R.J. (1990) Scanning tunneling microscopy observations on the reconstructed Au(111) surface – Atomic structure, long-range superstructure, rotational domains, and surface defects, *Phys. Rev. B* **42**, pp. 9307–9318.
18. Kern, K., Niehus, H., Schatz, A., Zeppenfeld, P., George, J. and Comsa G. (1991) Long-range spatial self-organization in the adsorbate-induced restructuring of surfaces – Cu(110)-(2×1)O, *Phys. Rev. Lett.* **67**, pp. 855–858.
19. Vanderbilt, D. (1992) Phase segregation and work function variations on metal surfaces – Spontaneous formation of periodic domain structures, *Surf. Sci.* **268**, pp. L300–L304.